Available online at www.cuijca.com

INTERNATIONAL JOURNAL OF COMPUTATIONAL ANALYSIS

Vol (5), No. (1), pp. 11-30

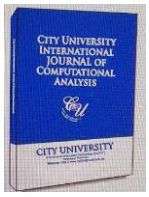

A TIME-FRACTIONAL MODEL FOR BRINKMAN-TYPE NANOFLUID WITH VARIABLE HEAT AND MASS TRANSFER

Atta Ullah[1], Afnan Ahmad[2]*, Umair Khan[3], Abdussamad[1]

[1]*Fundamental and Applied Sciences Department, Universiti Teknologi PETRONAS, 32610, Malaysia*

[2]*Civil and Environmental Engineering Department, Universiti Teknologi PETRONAS, 32610, Malaysia*

[3]*Mechanical Engineering Department, Universiti Teknologi PETRONAS, 32610, Malaysia*

**Corresponding Author: afnan_19001642@utp.edu.my*

Keywords:
Exact Solutions, Fourier's and Fiks Law's, Brinkman Type Fluid, Fractional Calculus

A B S T R A C T

Heat exchangers, vehicles, solar power production, and other thermal applications all make use of nanofluids. The next generation of fluids, known as nanofluids, have thermal characteristics that are superior to those of conventional fluids. A generalized Brinkman-type fluid model was created to predict the heat-transfer properties of an inclined solar collector using nanofluids under the influence of a transverse magnetic field. Additionally discussed are the effects of heat radiation and concentration. Furthermore, by using the extended Fick's and Fourier's Laws to transform classical governing equations into fractional partial differential equations, we apply the concept of Caputo time fractional derivative in this paper. The equations of energy and concentration are transformed with the help of new productive transform initial and boundary conditions. The Laplace and Fourier sine transforms are applied together and solve the transformed equations. The current study used a variety of nano-sized solid particles, including SWCNTs, and MWCNTs, and found that adding of MWCNTs to the water (working fluid) can increase the rate of heat transfer up to 34.84 per cent, improving the working ability of inclined solar collectors by increasing their solar radiation absorption power.

1 Introduction

Solar energy is now recognized widely as one of the extensive sources free, of clean, sustainable energy with less environmental effect. Energy demand expanded after the industrial revolution in the 1970s, pushing scientists to look for new sources of energy. Solar energy is usually regarded as the most environmentally friendly of all sustainable energy sources. Renewable energy sources may contribute to the worldwide electricity demand in recent years, with fossil fuels accounting for 40% [1-2]. Sun-derived energy is described as solar energy that can be transformed into heat and electricity. It is a natural consequence of the thermonuclear processes occurring inside the Sun's core emitting electromagnetic radiation. Due to this reason, it has been producing energy for billions of years. In the last ten years, solar energy has gained a lot of attention [3]. The expanding need for energy, the finite supply of fossil fuels, and the considerable environmental concerns linked with

them, particularly carbon dioxide emissions are the primary drivers of interest in solar energy applications. Furthermore, low thermal behaviour is an issue for energy conversion systems. Researchers suspended solid particles of nano-sized in a base fluid to overcome this difficulty and improve the efficiency of those working fluids which have poor thermal conductivities. Nanofluids are a new category of nanotechnology-focused heat transfer fluids made by distributing and maintaining nanoparticles ranging in size from 1 to 50 nanometers in conventional heat transfer fluids. Choi [4] coined the term "nanofluid" in 1995 to describe suspensions containing nanofluidic millimeter or micron-sized particles that have improved rheological properties, thermal properties, and thermal conductivity.

Nanoparticles are extensively applied in both biological and industrial fields. Similarly, the field of energy nanoparticles has inspired a lot of interest. Nanoparticles are very helpful in the processes of energy conversion like thermoelectric devices, and solar and fuel cells. Nanoparticles are very essential in devices that are used for the storage of energy such as capacitors and rechargeable batteries. Furthermore, nanoparticles are used in insulating objects like aerogels, glazes, and powerful lightning including light and organic light-emitting diodes. Nanofluids have shown the capability in improving heat transfer in a wide range of applications, including industrial transportation, nanoelectromechanical systems, refrigeration, nuclear reactors, micro-electromechanical systems, electronics, and biomedical equipment [5, 6]. Thermal conductivity can be increased to improve performance and reduce operating costs. Increasing thermal conductivity has been shown to improve performance and lower operating costs [7], and further related research can be found in [8–11]. Different experts examine the influence of distinct schemes on the forced and natural convection of nanofluid flows [12–16]. Nanofluids have the potential to enhance the thermodynamic properties of the fluid, which is very essential in industries, particularly in the cooling and heating of solar thermal systems. Nanofluidics can play a vital role in manufacturing i.e manufacture crucial nanostructured objects and clean surfaces in complex fluid engineering because of their exceptional wettability and dispersion qualities [17]. The administration of nanomedicine is another usage of nanofluids, as evidenced in [18]. Nanofluids with large thermal conductivity are very decisive for reducing plugging the walls in transport mediums, increasing energy productivity, improving execution, and lowering costs [19]. In Tocrease the efficiency of energy, Hussanan et al. [20] examined the microinertia and microrotation impacts of a stream of nanoparticles in motor oil, kerosene oil, and water. Tesfai et al. [21], investigated the grapheme oxide suspension and thermal execution of graphene in an experimental study. They investigated the rheological properties as well as the inherent viscosity in the suspension of Gragrapheneli et al. [22], and found precise results for a Brinkman-type fluid flow including various microparticles by using the Laplace transform approach, they were able to achieve exact solutions. An article based on the uses of particles in the field of engineering was presented by Wu and Zhao [23]. According to this particular article, the author has described the importance of critical heat flux and heat transfer. Khan [24], has examined the effect of various-shaped nanoparticles in the base fluid on the heat transfer rate enhancement. The numerical results obtained related to the flow of the fluid along with nanoparticles were calculated using the finite difference approach of Sheikholislami and Bhatti [25]. The improvement in heat transmission due to nanoparticles was briefly discussed in this article. Rashidi et al. [26], investigated how a magnetic field affected the flow of a generalized Burgers' nanofluid along an inclined wall. Mahian et al. [27], discuss the performance of solar stills employing nanofluid. The author has provided both the results, theoretical and experimental in this paper. Similarly, the concise review

of a nanofluid along with its applications was resented by Kasaeian et al. [28]. A solar collector is a device that exchanges heat, which converts solar energy to a transport medium's internal energy.

These types of equipment allow energy from the sun and then convert it to the form of heat and after that transmit that heat to the collecting fluid, mostly oil, air, and water. The energy stored in the working fluid can be transmitted directly to air or water conditioning device, as well as thermal storage reservoirs for use at night or in overcast weather. [29]. Solar collectors are one of the most essential devices of solar energy. In a review paper, Mahian et al. [30], studied the use of nanofluids to improve the capability of solar water heaters and solar collectors. This research paper also includes impacts on environmental and economic concerns. Using the Laplace transform approach, Sheikh et al. [31], were able to get the closed-form solution for the generalized fluid flow. They concluded that adding nanoparticles to the base fluid can improve the performance of solar collectors. Furthermore, the regulation of heat transmission via sloped or corrugated walls necessitates the use of a solar collector or natural convection of the roof. The field of the temperature and flow are very complicated with these complex geometries shown in (Fig.1) [32]. Fan et al. [33], illustrated the transfer of heat and flow dissemination in a solar collector with an inclined strip shelter. The performance of solar collectors has been studied both theoretically and practically. Hatami et al. [34], applied the finite difference approach and develop some important results for a solar collector numerically with an inclined plate. They observed that increasing the maximum volume fraction of nanoparticles in a solar collector can improve its efficiency.

There are two most often concepts are used in fractional differentiation and integration in applied mathematics nowadays. Due to filtering and memory effects can be included in ordinary differential equations (ODE's) or partial differential equations PDE's to model real-world issues [35]. Different sorts of non-integer order derivatives have recently been used in the literature. Among these, the Riemann-Liouville derivative is the most widely used fractional derivative [36].

However, there are several extensive defects in the utilization of Riemann-Liouville derivatives, such as the fact that the derivative of a constant value is not zero. To address the Riemann-Liouville derivative's deficiency, Caputo [37] presented an improved form of the derivative in non-integer order, familiar with the Caputo derivative in literature. Caputo derivatives on the physical system were successfully applied such as electro hysteresis, damage, viscoelasticity, and fatigue [38]. Caputo used this attitude and solve many problems of elasticity. After Caputo, several researchers like Friedrich [39], and Ali et al. [40], used the Caputo approach and got some interesting solutions.

With the above discussion in mind, the goal of this research is to look into the effects of nanoparticles (MWCNTs, SWCNTs, and) on the working fluid's heat and mass transfer rate, as well as their prospective applications in solar collectors with inclined plates. With the use of generalized Fourier's and Fick's Laws, the governing equations are converted to fractional PDEs utilizing the idea of Caputo time fractional derivative (CFD). The energy and concentration equations are transformed using the initial and boundary conditions using a newly devised transformation. The integral transforms namely Laplace and Fourier sine transforms are combined and used to solve the transformed equations. The solutions are presented in graphs and tables and satisfy all of the physical conditions.

2. Mathematical Modelling

In the present problem, an incompressible generalized Brinkman-type fluid in the inclined channel with the impact of thermal radiation is considered. The fluid motion is considered along the x-axis. The fluid occupies the space $y > 0$ between

inclined channels. In the existence constant magnetic field, fluid will be considered electrically conducting. Along the flow of fluid the applied magnetic field, will be in the transverse direction. At the time $t = 0^+$ both plates and fluid are at rest with ambient concentration and temperature respectively. The velocity of the plate becomes when the time the plate is at starting motion in its own plane which is clear from Fig.1. The concentration and temperature level increased respectively with respect to the time when the plate is at $y = d$. Fig.1. shows the problem geometry.

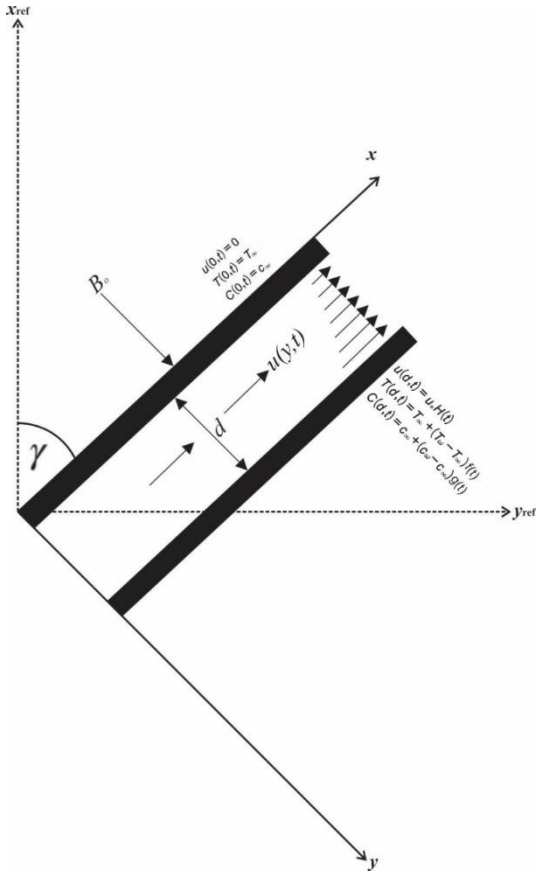

Fig. 1: Physical geometry of the flow

By considering the above points and assumptions the Boussinesq's approximation, governing equations can be written as:

$$\frac{\partial u}{\partial t} + \beta u = \frac{\mu_{nf}}{\rho_{nf}} \frac{\partial^2 u}{\partial y^2} - \frac{\sigma_{nf}}{\rho_{nf}} B_0{}^2 u + \frac{\vec{g}\left(\rho\beta_T\right)_{nf}}{\rho_{nf}}\left(T - T_\infty\right)\cos\gamma + \frac{\vec{g}\left(\rho\beta_C\right)_{nf}}{\rho_{nf}}\left(C - C_\infty\right)\cos\gamma, \tag{1}$$

The initial constraints are as under:

$$\frac{\left(\rho_{C_p}\right)_{nf}}{\partial t}\frac{\partial T\left(y,t\right)}{\partial t} = K_{nf}\frac{\partial^2 T\left(y,t\right)}{\partial y^2} - \frac{\partial q_r}{\partial y}, \tag{2}$$

$$\frac{\partial C(y,t)}{\partial t} = -\frac{\partial \gamma(y,t)}{\partial y}, \tag{3}$$

$$\gamma(y,t) = -D_{nf}\,\frac{\partial C(y,t)}{\partial y}. \tag{4}$$

The boundary and initial conditions are given below.

$$\left.\begin{aligned} u(y,0) = 0,\ \ \mathrm{T}(y,0) = T_\infty,\ \ \mathrm{C}(y,0) = C_\infty,\\ u(0,t) = 0,\ \ \mathrm{T}(0,t) = T_\infty,\ \ \mathrm{C}(0,t) = C_\infty,\\ u(d,t) = u_0\mathrm{H(t)},\ \ \mathrm{T(d\ ,t)} = T_\infty + (T_w - T_\infty)\,f\left(t\right),\\ \mathrm{C(d\ ,t)} = C_\infty + (C_w - C_\infty)g\left(t\right), \end{aligned}\right\}. \tag{5}$$

The expressions ρ_{nf}, μ_{nf}, σ_{nf}, $(\rho\beta_T)_{nf}$, k_{nf} and $(\rho\beta_C)_{nf}$ for nanofluids can be defined as [41],

$$\left\{\begin{aligned} &\rho_{nf} = (1-\phi)\rho_f + \phi\rho_s,\ \ \mu_{nf} = \mu_f\,(1-\phi)^{-2.5},\ \ (\rho\beta_T)_{nf} = (1-\phi)(\rho\beta_T)_f + \phi(\rho\beta_T)_s,\\ &k_{nf} = k_f\left[\frac{1-\phi+2\phi\left(\frac{k_s}{k_s-k_f}\right)ln\frac{k_s+k_f}{2k_f}}{1-\phi+2\phi\left(\frac{k_f}{k_s-k_f}\right)ln\frac{k_s+k_f}{2k_f}}\right], \qquad (\rho\beta_C)_{nf} = (1-\phi)(\rho\beta_C)_f + \phi(\rho\beta_C)_s,\\ &\sigma_{nf} = \sigma_f\left[1+\frac{3(\sigma-1)\phi}{(\sigma+2)-(\sigma-1)\phi}\right], \qquad D_{nf} = (1-\phi)D_f. \end{aligned}\right\} \tag{6}$$

Table 1. Thermo-physical characteristics of nanoparticles and water.

Properties	ρ	C_p	K	β	Pr
H_2O	997.1	4179	0.613	21	6.2
SWCNT	2600	425	6600	27	-
MWCNT	1600	796	3000	44	-
CuO	8933	385	401	1.67	-
TiO_2	4250	686.2	8.95928	0.9	-

In the current work, Roseland's approximation can be used for radiation flux q_r as:

$$q_r = \frac{-4\sigma^*}{3k^*}\frac{\partial T^4}{\partial y}. \quad (7)$$

A slight diversity in the temperature between T and T_∞ is imagine, by applying the Taylor expansion series for the current temperature T_∞ and T^4 can be linearized. Ignoring higher-order and second order terms in ($T - T_\infty$), we obtained:

$$T^4 = 4T_\infty{}^3\mathrm{T} - 3T_\infty{}^4.$$

Using the above in Eq. (7), we obtained:

$$q_r = \frac{-4\sigma^*}{3k^*}\frac{\partial\left(4T_\infty{}^3\,\mathrm{T} - 3T_\infty{}^4\right)}{\partial y}.$$

Hence $\frac{\partial T_\infty{}^4}{\partial y} = 0$, because $T_\infty{}^4$ is a constant temperature and as a result we get the following equation.

$$q_r = \frac{-16T_\infty{}^3\sigma^*}{3k^*}\frac{\partial T}{\partial y}. \quad (8)$$

By putting Eq. (8) in Eq. (2), we have

$$\left(\rho c_p\right)_{nf}\frac{\partial T}{\partial t} = k_{nf}\frac{\partial^2 T}{\partial y^2} + \frac{16T_\infty{}^3\sigma^*}{3k^*}\frac{\partial^2 T}{\partial y^2}. \quad (9)$$

By using the following dimensionless variables:

$$\xi = \frac{y}{d},\quad \tau = \frac{\nu}{d}t,\quad \theta = \frac{T - T_\infty}{T_w - T_\infty},\quad \phi = \frac{C - C_\infty}{C_w - C_\infty},\quad v = \frac{u}{u_0},\quad \delta = \frac{\gamma d}{D_{nf}(C_w - C_\infty)}.$$

Eqs. (10), (11) and (13) are dimensionless forms of Eqs. (1), (9) and (3) respectively.

$$\frac{\partial v(\xi,\tau)}{\partial\tau} + \beta_1 v(\xi,\tau) = \phi_5\frac{\partial^2 v(\xi,\tau)}{\partial\xi^2} - Mv(\xi,\tau) + Gr_0\theta(\xi,\tau)\cos\gamma + Gm_0\phi(\xi,\tau)\cos\gamma, \quad (10)$$

$$\frac{\partial\theta(\xi,\tau)}{\partial\tau} = \frac{1}{Pr_{eff}}\frac{\partial\lambda(\xi,\tau)}{\partial\xi}. \quad (11)$$

Where

$$\lambda(\xi,\tau) = \frac{\partial\theta(\xi,\tau)}{\partial\xi},$$

Similarly

$$\frac{\partial \phi(\xi,\tau)}{\partial \tau} = -\frac{1}{a_0}\frac{\partial \delta(\xi,\tau)}{\partial \xi}, \tag{12}$$

Where

$$\delta(\xi,\tau) = -\frac{\partial \phi(\xi,\tau)}{\partial \xi}.$$

The following are the dimensionless boundary and initial conditions

$$\begin{aligned} &v(\xi,0) = 0 && \theta(\xi,0) = 0 && \phi(\xi,0) = 0 \\ &v(0,\tau) = 0 && \theta(0,\tau) = 0 && \phi(0,\tau) = 0 \\ &v(d,\tau) = h(\tau), && \theta(d,\tau) = f(\tau), && \phi(d,\tau) = g(\tau), \end{aligned} \tag{13}$$

where

$$Gr = \frac{d^2 g\beta_{Tf}(T_w - T_\infty)}{u_0 \nu},\ Gm = \frac{d^2 g\beta_{Cf}(C_w - C_\infty)}{u_0 \nu},\ M = \frac{d^2 \sigma_f \mathrm{B}^2{}_0}{\rho_f \nu},\quad Pr = \frac{(\mu_{Cp})_f}{k_f},\quad Sc_0 = \frac{\nu}{D_f},$$

represent thermal Grashof number, mass Grashof number, magnetic parameter, Prandtl number, and Schmidt number respectively.

3. Fractional model

For the above specified problem we construct a fractional model, by applying generalized Fick's and Fourier's law's on Eqs. (11) and (12), we obtained:

$$\theta(\xi,\tau) = -{}^{C}D_{\tau}^{1-\alpha}\left(\frac{\partial \lambda(\xi,\tau)}{\partial \xi}\right):\ 0 < \alpha \le 1, \tag{14}$$

$$\phi(\xi,\tau) = -{}^{C}D_{\tau}^{1-\alpha}\left(\frac{\partial \delta(\xi,\tau)}{\partial \xi}\right):\quad 0 < \alpha \le 1. \tag{15}$$

The Caputo time fractional operator ${}^{C}D_{\tau}^{\alpha}(.)$ can be define as [42].

$${}^{C}D_{t}^{\alpha} r(y,t) = \frac{1}{\Gamma(1-\alpha)}\int_0^t r(y,s)(t-s)^{-\alpha}\,ds = \eta_\alpha(t) * r(y,t):\ 0 < \alpha \le 1. \tag{16}$$

Where, $\eta_\alpha(t) = \dfrac{t^{-\alpha}}{\Gamma(1-\alpha)}$. Moreover,

$$L\{\eta_\alpha(t)\} = \frac{1}{s^{1-\alpha}},\ \{\eta_{1-\alpha} * \eta_\alpha\}(t) = 1,\ \eta_0(t) = L^{-1}\left\{\frac{1}{s}\right\} = 1,\ \eta_1(t) = L^{-1}\{1\} = \xi(t). \tag{17}$$

By applying the mentioned identities and 2nd part of Eq. (16), it is a conventional tendency to indicate that

$$ {}^{C}D_t^{0} r(y,t) = r(y,t) - r(y,0) \tag{18}$$

$$ {}^{C}D_t^{1} r(y,t) = \frac{\partial r(y,t)}{\partial t} \tag{19}$$

Using the Caputo time fractional (CF) operator and Eqs. (11), (12), (14) and (15) respectively:

$$ \frac{\partial \theta(\xi,\tau)}{\partial t} = \frac{1}{Pr_{eff}} {}^{C}D_{\tau}^{1-\alpha} \left(\frac{\partial^2 \theta(\xi,\tau)}{\partial \xi^2} \right) \tag{20}$$

$$ \frac{\partial \phi(\xi,\tau)}{\partial t} = \frac{1}{a_0} {}^{C}D_{\tau}^{1-\alpha} \left(\frac{\partial^2 \phi(\xi,\tau)}{\partial \xi^2} \right). \tag{21}$$

Equations (20) and (21) can also be written as follows:

$$ \Im_t^{1-\alpha} r(y,t) = (\eta_{\alpha} * r)(t) = {}^{C}D_t^{\alpha} r(y,t), $$

$$ {}^{C}D_{\tau}^{\alpha} \theta(\xi,\tau) = \frac{1}{Pr_{eff}} \frac{\partial^2 \theta(\xi,\tau)}{\partial \xi^2}, \tag{22}$$

$$ {}^{C}D_{\tau}^{\alpha} \phi(\xi,\tau) = \frac{1}{a_0} \frac{\partial^2 \phi(\xi,\tau)}{\partial \xi^2}. \tag{23}$$

4. Solution of the problem

The above fractional model has been solved using the Laplace and Fourier transformation jointly.

4.1 Solution of the Energy Equation

Applying the following transformation

$$ \chi(\xi,\tau) = \theta(\xi,\tau) - \xi f(\tau). \tag{24}$$

Equation (22), can be written as:

$$ {}^{C}D_{\tau}^{\alpha} \chi(\xi,\tau) + \xi {}^{C}D_{\tau}^{\alpha} f(\xi,\tau) = \frac{1}{Pr_{eff}} \frac{\partial^2 \chi(\xi,\tau)}{\partial \xi^2}. \tag{25}$$

The corresponding form of boundary and initial conditions can be written as:

$$ \chi(\xi,0) = 0, \qquad \chi(0,\tau) = 0, \qquad \chi(1,\tau) = 0. \tag{26}$$

We get Eq. (27) by using Fourier sine and Laplace transforms:

$$\bar{\chi}_F(n,s) = s\bar{f}(s)\frac{(-1)^n}{n\pi}\frac{s^{\alpha-1}}{s^\alpha + \frac{(n\pi)^2}{Pr_{eff}}}. \tag{27}$$

We get Eq. (28) by inverting Eq. (27) with the help of integral transformations:

$$\chi(\xi,\tau) = 2\sum_{n=1}^{\infty}\frac{(-1)^n}{n\pi}\sin(n\pi\xi)\int_0^\tau f(\tau-t)\mathrm{E}_{\alpha,\alpha-1}\left(\frac{-(n\pi)^2}{Pr_{eff}}t^\alpha\right)dt. \tag{28}$$

Hence, the solution of the equation of energy is as under:

$$\theta(\xi,\tau) = \chi(\xi,\tau) + \xi f(\tau).$$

4.2 Solution of concentration profile

By applying the transformation:

$$\psi(\xi,\tau) = \phi(\xi,\tau) - \xi g(\tau). \tag{29}$$

Equation. (23) can be written as:

$${}^{C}D_{\tau}^{\alpha}\psi(\xi,\tau) + \xi\,{}^{C}D_{\tau}^{\alpha}g(\tau) = \frac{1}{a_0}\frac{\partial^2\psi(\xi,\tau)}{\partial\xi^2}. \tag{30}$$

The corresponding form of boundary and initial conditions can be written as

$$\psi(\xi,0) = 0, \quad \psi(0,\tau) = 0, \quad \psi(1,\tau) = 0. \tag{31}$$

We get Eq. (32) by using the mentioned integral transformations (Laplace and Fourier sine transform):

$$\bar{\psi}_F(n,s) = s\bar{g}(s)\frac{(-1)^n}{n\pi}\frac{s^{\alpha-1}}{s^\alpha + \frac{(n\pi)^2}{a_0}}. \tag{32}$$

We get Eq. (33) by taking the inverse transformation of Eq. (32):

$$\psi(\xi,\tau) = 2\sum_{n=1}^{\infty}\frac{(-1)^n}{n\pi}\sin(n\pi\xi)\int_0^\tau g(\tau-t)\mathrm{E}_{\alpha,\alpha-1}\left(\frac{-(n\pi)^2}{a_0}t^\alpha\right)dt. \tag{33}$$

For the concentration equation the last solution is:

$$\phi(\xi,\tau) = \psi(\xi,\tau) + \xi g(\tau). \tag{34}$$

4.3 Solution of velocity profile

By transforming Eq. (10) with the help of Fourier and Laplace transformations and using Eq. (13), we obtained:

$$\bar{v}_F(n,s)=\frac{(-1)^{n+1}}{n\pi}\bar{h}(s)+\left(\frac{L_3}{s}+\frac{L_2}{s+L_1}\right)\frac{(-1)^n s\bar{h}(s)}{n\pi}+\frac{Gr_0\cos\gamma}{s+L_1}\left\{\frac{(-1)^n s\bar{f}(s)}{n\pi}\frac{s^{\alpha-1}}{s^\alpha+\frac{(n\pi)^2}{Pr_{eff}}}+\frac{1}{s^2}\frac{(-1)^{n+1}}{n\pi}\right\}$$

$$+\frac{Gm_0\cos\gamma}{s+L_1}\left\{\frac{s\bar{g}(s)(-1)^n}{n\pi}\frac{s^{\alpha-1}}{s^\alpha+\frac{(n\pi)^2}{a_0}}+\frac{1}{s^2}\frac{(-1)^{n+1}}{n\pi}\right\}. \tag{35}$$

where

$$L_1=H+\phi_5(n\pi)^2,\ H=M+\beta_1,\ M=\frac{d^2\delta_f B^2{}_0}{\rho_f\nu},\ \beta_1=\frac{\beta d^2}{\nu},\ L_2=\frac{\phi_5(n\pi)^2}{L_1},\ L_3=1-L_2.$$

By applying the inverse Fourier sine and Laplace transformations, we get the solution as under:

$$v(\xi,\tau)=\xi h(\tau)+2\sum_{n=1}^{\infty}\frac{(-1)^n}{n\pi}h(\tau)*\left(h(\tau)L_3+L_2\exp(-L_1)\right)\sin(n\xi\tau)$$

$$+2Gr_0\cos\gamma\sum_{n=1}^{\infty}\exp(-L_1)\frac{(-1)^n}{n\pi}*\left\{\int_0^\tau f(t-\tau)\mathrm{E}_{\alpha,\alpha-1}\left(\frac{-(n\pi)^2}{Pr_{eff}},\tau\right)d\tau+\tau f(\tau)\right\}\sin((n\pi\xi) \tag{36}$$

$$+2Gm_0\cos\gamma\sum_{n=1}^{\infty}\exp(-L_1)\frac{(-1)^n}{n\pi}*\left\{\int_0^\tau g(t-\tau)\mathrm{E}_{\alpha,\alpha-1}\left(\frac{-(n\pi)^2}{a_0},\tau\right)d\tau+\tau g(\tau)\right\}\sin((n\pi\xi).$$

4.4 Nusselt number

For the Nusselt number of Brinkman-type Nanofluid (BTNF) the mathematical expression is written as:

$$Nu=-\frac{k_{nf}}{kf}\frac{\partial\theta(\xi,\tau)}{\partial\xi}\bigg|_{\xi=0}. \tag{37}$$

4.5 Sherwood number

For the Sherwood number of Brinkman-type Nanofluid (BTNF) the mathematical expression is written as:

$$S_h=-D_{nf}\frac{\partial\phi(\xi,\tau)}{\partial\xi}\bigg|_{\xi=0}. \tag{38}$$

5. Results and discussion

In the current article, we discussed the unsteady flow of generalized Brinkman-type nanofluid in an inclined channel. The effect of mass and heat transfer have been considered combinedly. By applying the generalized Fourier's and Fick's laws a fractional model has been constructed. The integral transforms i.e Fourier sine and Laplace are employed to achieve the solutions in closed form. Tables and figures show the impact of various embedded parameters on temperature, concentration and velocity profiles. To know the problem in-depth, we discussed the impact of various nanoparticles like, (MWCNTs, SWCNTs, TiO_2 and CuO), in base fluid (water), which have been portrayed in Fig. 2. It is observed that the base fluid velocity with MWCNTs is analogously smaller than the velocity of water with SWCNTs, TiO_2 and CuO because of the higher thermal conductivity and density of MWCNTs. The MWCNTs-water nanofluid becomes denser when MWCNTs are spread in water than the nanofluid having (SWCNTs, TiO_2 and CuO). Consequently, the base fluid (water) with nanoparticles (SWCNTs, TiO_2 and CuO) has less viscosity as compared to MWCNTs with working fluid (water). As a result, the working fluid's boiling point (water with MWCNTs) is greater than the working fluid's boiling point (water with SWCNTs, TiO_2 and CuO). Moreover, the heat absorption and heat flow capability of inclined solar collectors will significantly increase and also the more viscous fluid have a low freezing point. Simply we can say that, the freezing point of the working fluid might be regulated at very low temperatures by adding MWCNTs. The current observation also complies with the experimental study done by He et al. [42], where they noticed the effect of TiO_2 and CNTs on vacuum tube solar collectors and also find out that water-based CNTs nanofluids are better than water-based TiO_2 nanofluids.

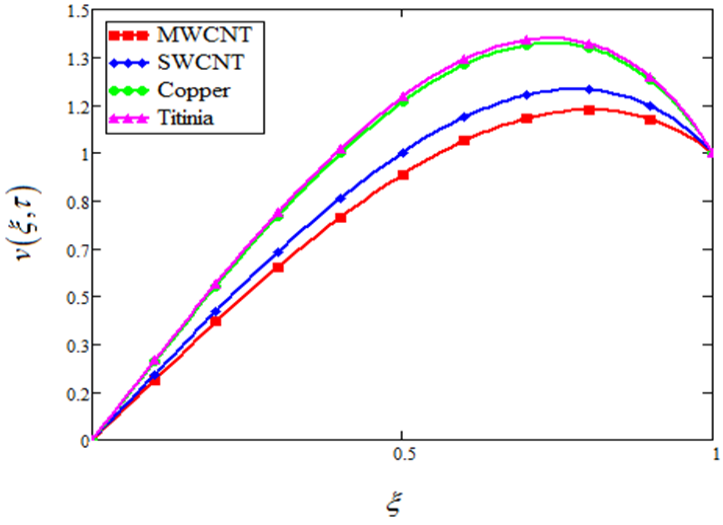

Fig.2. Change in velocity profile due to different nanoparticles.

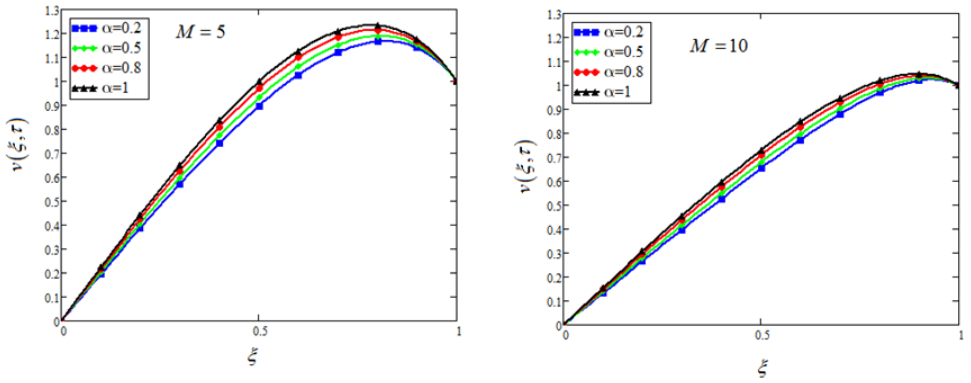

Fig.3. Change in velocity profile due to various values of M when $\beta = 0.5,\ Gm = 0.5,$

$$\varphi = 0.01,\ Nr = 0.2,\ Sc = 0.2,\ Gr = 0.5,\ \gamma = \frac{\pi}{4}.$$

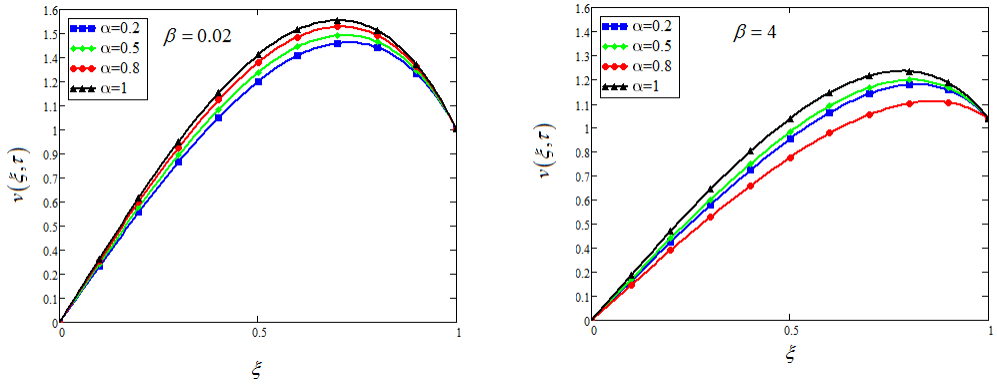

Fig.4. Change in velocity due to various values of β when $Nr = 0.2, Gm = 0.5,$

$$Gr = 0.5,\ \varphi = 0.01,\ M = 2.5, Sc = 0.2,\ \gamma = \frac{\pi}{4}.$$

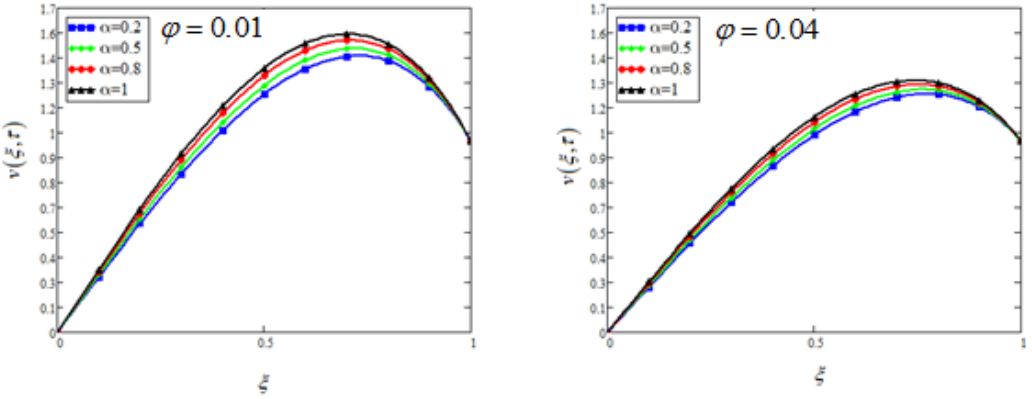

Fig.5. Change in velocity due to various values of φ when $Nr = 0.2,\ \beta = 0.5,\ t = 1,$

$$M = 2.5,\ Gm = 0.5,\ Sc = 0.2,\ Gr = 0.5,\ \gamma = \frac{\pi}{4}.$$

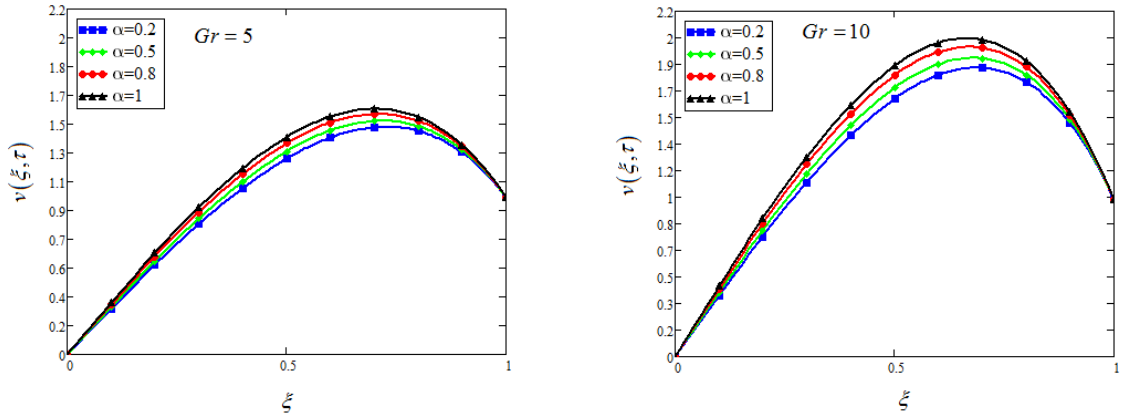

Fig.6. Change in velocity due to various values of Gr when $t=1,\ \beta=0.5,\ Nr=0.2,$

$M=2.5,\ \varphi=0.01,\ Sc=0.2,\ Gm=0.5,\ \gamma=\frac{\pi}{4}.$

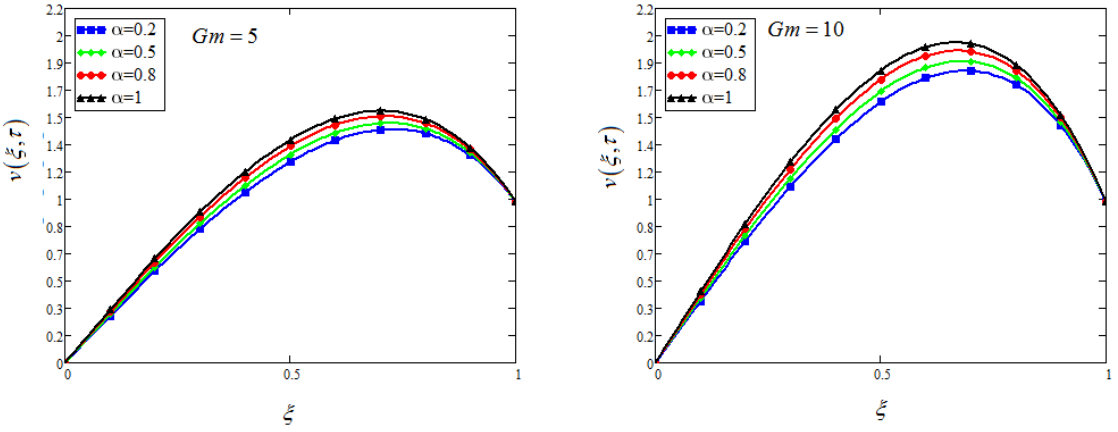

Fig: 7. Change in velocity due to various values of Gm when $t=1,\ \beta=0.5,$

$M=25,\ Nr=0.2,\ \varphi=0.01,\ Gr=0.5,\ Sc=0.2,\ \gamma=\frac{\pi}{4}.$

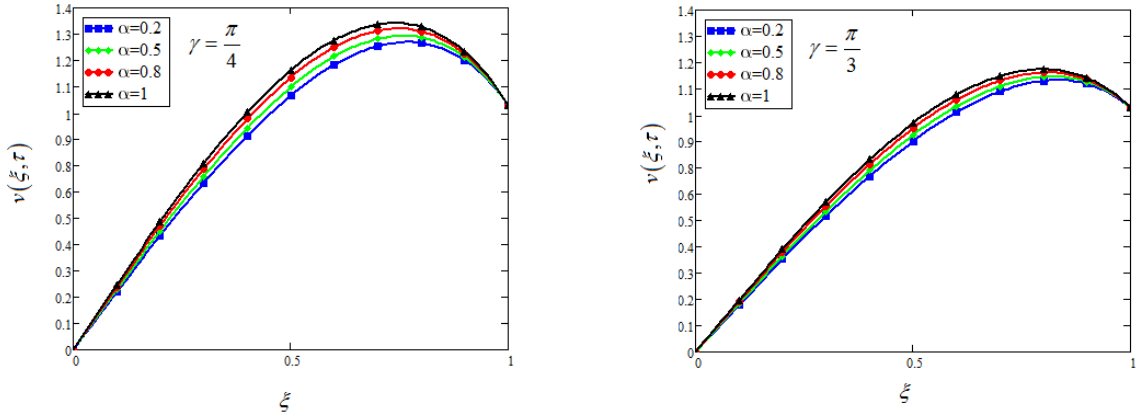

Fig.8. Change in velocity profile due to various values of γ when $t=2,\ \beta=0.5,$

$\varphi=0.01,\ Gr=0.5,\ Sc=0.2,\ M=2.5,\ Nr=0.2,\ Gm=0.5.$

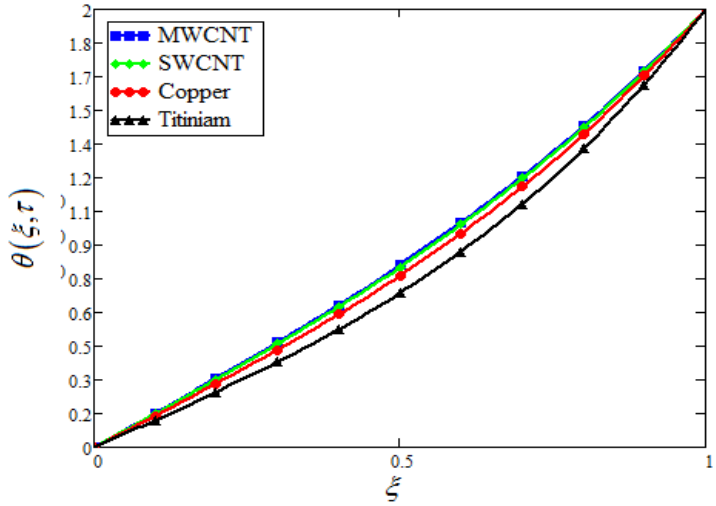

Fig.9. Change in the profile of temperature due to various nanoparticles.

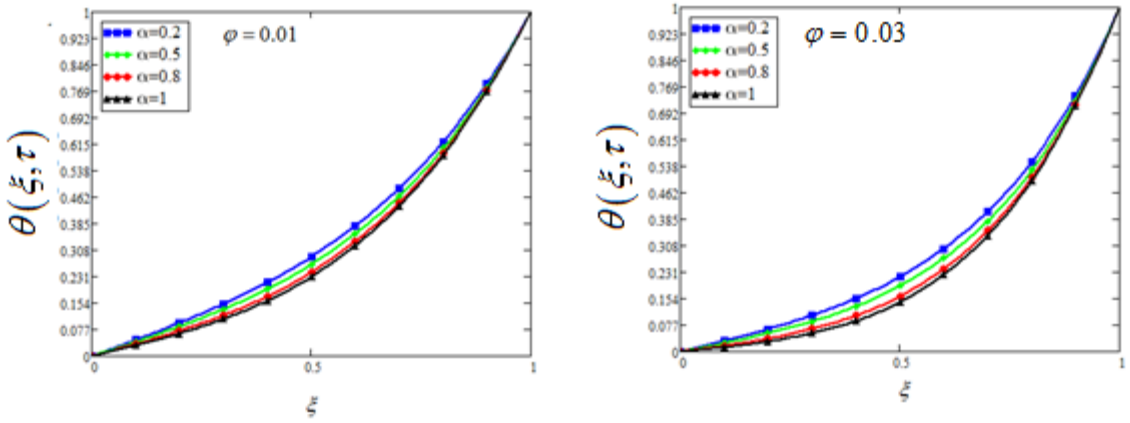

Fig.10. Change in the profile of temperature due to various values of φ when $t = 1,\ Nr = 0.2,\ Pr = 6.2.$

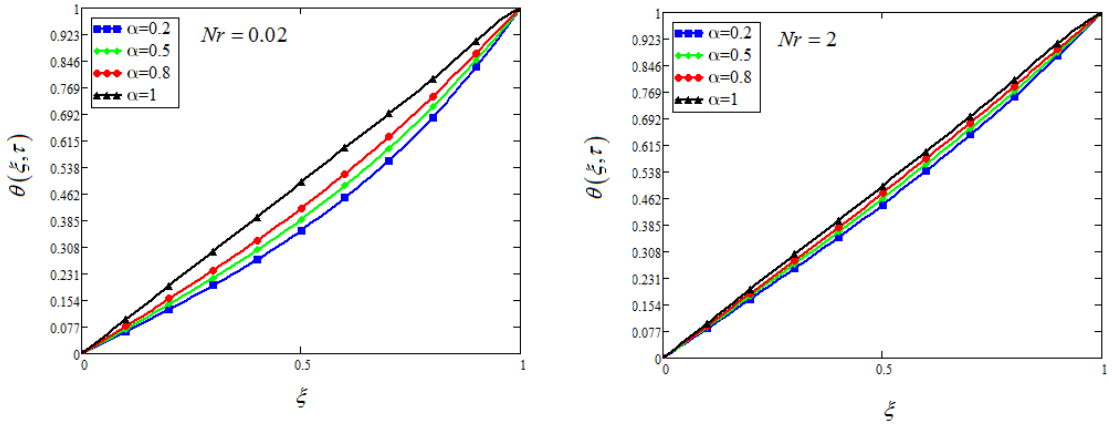

Fig.11. Change in the profile of temperature due to various values of Nr when $t = 1,\ pr = 6.2,\ \varphi = 0.01.$

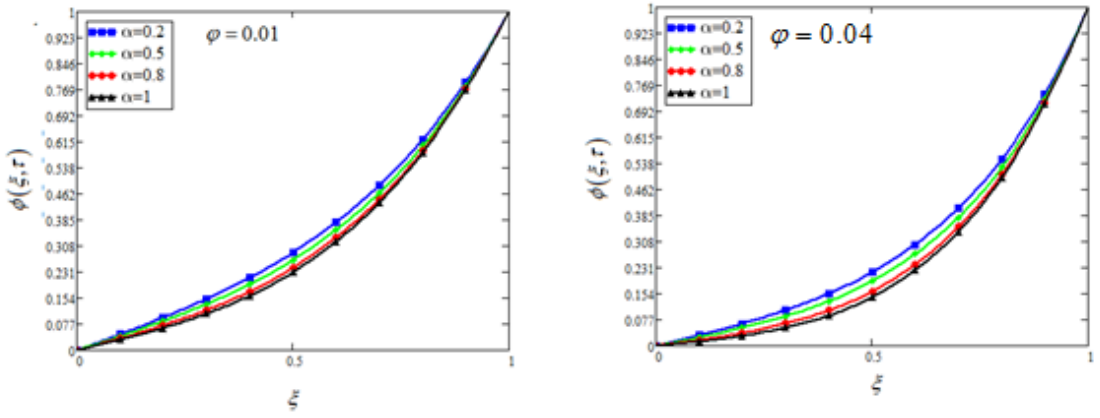

Fig.12. Change in the profile of concentration due to various values of φ when $t = 1,\ Sc = 0.2.$

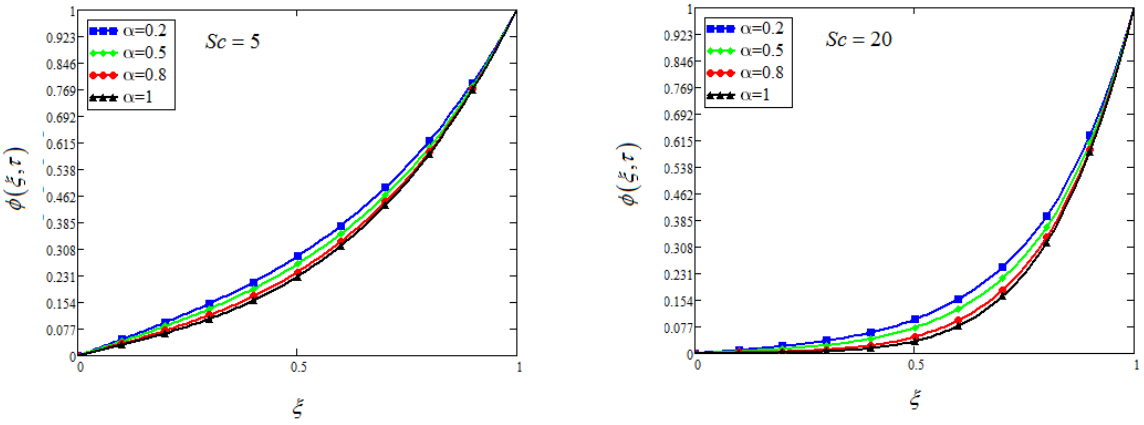

Fig.13. Change in the profile of concentration due to various values of Sc when $t = 2,\ \varphi = 0.01.$

Table 2. For various nanoparticles, effect on Sherwood number of different parameters.

α	Sc	φ	S_h
0.2	5.0	0.02	1.105
0.3	5.0	0.02	1.072
0.2	**10**	0.02	0.579
0.2	5.0	**0.04**	1.066

Table 3. For various nanoparticles, effect on Nussle number of different parameters.

φ	α	Nr	$MWCNT$	$SWCNT$	CuO	$TiO2$
0.00	0.2	0.2	0.485	0.485	0.485	0.485
0.01	0.2	0.2	0.533	0.526	0.519	0.507
0.02	0.2	0.2	0.573	0.565	0.558	0.543
0.03	0.2	0.2	0.609	0.601	0.592	0.581
0.04	0.2	0.2	0.654	0.639	0.634	0.623
0.01	0.5	0.2	0.522	0.518	0.513	0.502
0.01	0.7	0.2	0.517	0.513	0.507	0.495
0.01	1	0.2	0.512	0.508	0.501	0.489
0.01	0.2	0.4	0.564	0.539	0.531	0.521

Table 4. Enhancement of Heat transfer for various volume fractions

φ	$MWCNT$ %	$SWCNT$ %	CuO %	TiO_2 %
0.00	--	--	--	--
0.01	9.89	8.45	7.01	4.53
0.02	18.14	16.49	15.05	11.95
0.03	25.56	23.91	22.06	19.79
0.04	34.84	31.75	30.72	28.45

The effect of the magnetic parameter M on the velocity profile is shown in Fig. 3. Which shows that there is inverse variation between velocity and magnetic parameter because when the values of magnetic parameter M is increasing a decrease occurs in the velocity. Physically, larger values of M rise the resistive forces (Lorentz forces), because of which the fluid velocity decreases. Fig. 4 shows the effect of the Brinkman parameter β. A decrease in velocity can be observed by taking greater values of β. It is shown that the fluid velocity is greater at $\beta = 0.02$ and lesser at $\beta = 4$. Physically, this is correct, since the parameter of Brinkman β is a ratio of drag forces to density. As drag forces increase, velocity decreases. The effect of nanoparticle volume fraction φ on velocity profile is depicted in Figure 5. The nanoparticle volume fraction φ is studied in the range of $0 \le \varphi \le 0.04$, due to sedimentation occurrence, when φ exceeds 0.08. Consequently, an increase in nanoparticles volume fraction φ bring a decrease in the velocity profile. Figs.6 and 7, show the effect of thermal

and mass Grashof numbers. These graphs indicate that as the increment occurs in Gm and Gr the velocity rises as well. The reason behind this fact is the buoyancy forces, which become more dominating, as the values of Gm and Gr increase therefore, as a result, shortening occurs in the thickness of the boundary layer. Fig. 8 portrayed the behaviour of the angle of inclination γ and this graph shows that when the value of γ grew higher, the fluid velocity decreased. Physically, larger values of γ reduce the bouncy effect in the flow, therefore the fluid's velocity also decreases [43]. Consequently, the fluid will be more viscous, and the solar collector's efficiency may be improved, as previously described.

The discrepancy in the profile of temperature for various types of nanoparticles has shown in Figure 9. From Fig. 9, it is clear that the profile of temperature is very high for MWCNT and low for (SWCNT, CuO and TiO_2) with base fluid respectively. Fig.10. shows increasing behaviour on temperature distribution for the increasing values of φ. The reason behind this behaviour is thermal conductivity which can be clarified from Eq. (6). The conduction of heat is based on the effective thermal conductivity, so, by increasing the thermal conductivity the conduction of heat is also increasing which brings the increment in the temperature distribution. It can be found in Fig. 11, that Nr have a similar effect on the temperature profile. Similarly, Figs.12 and 13, depict the impact of φ and Sc on the concentration equation. It is cleared from these figures that the concentration of mass is decreasing function for higher values of φ and Sc.

From table. 2, it is cleared that Sc is the ratio of mass diffusivity and viscous force, which gives enhancement in drag forces and hence the increment take place in Sherwood number. For various nanoparticles the effect of φ, Nr and φ versus Nusselt number is tabled in table 3. For higher values of φ and Nr an improvement can be observed in the Nusselt number while on the Nusselt number fractional parameter α has a reverse effect. From the table it is also observed that the MWCNTs-water nanofluid presents the maximum disparity in the Nusselt number pursue by other nanoparticales. In table 4 the impact of the volume fraction of various nanoparticles on the heat transfer rate has been illuminate. From the table it is clear that the heat transfer rate is maximum for value $\varphi = 0.04$. It is also clear and can be noted that the heat transfer rate of water has been grow up by 34.84% with MWCNTs, but on the other side 31.75%, 30.72% and 28.45% with SWCNTs, CuO and TiO_2 nanoparticles, respectively.

5 Conclusion

The efficiency of solar collectors will be sufficiently increased by using nanoparticles in the water (base fluid), as it is cleared from the theoretical and numerical results. The heat transfer in the rate of MWCNTs water-based nanofluid is greater than the heat transferring rate of SWCNTs, TiO_2 and CuO water based nanofluid. Hence nanofluids are denser than general fluids, which is why the boiling point is higher than the general basic fluids (water). Due to this, the efficiency of solar collectors will be increased. The higher viscosity of fluid leads to an inferior freezing point of fluids, and the point of freezing of solar cells will be controlled at a very small temperature by adding nanoparticles. A decrease in the bouncy effect will be observed by increasing values of γ. Hence, the fluid becomes more viscous so the fluid velocity will be decreased and the efficiency of the solar collector will be improved. For the fractionalization of the model, we use the generalized Fick's and Fourier's law to obtain the final solution and then a new transformation is applied to solve the model by using the integral

transforms that are Fourier and Laplace. The obtained results can be shown in tables and graphs. The key points of the current study are

- For the solution of the fractional model, the new transformation is authentic. By applying this transformation it is easier to obtain the solution of the fractional model.
- The use of MWCNTs increases the heat flowing rate of the working fluid (H_2O) by up to 34.84%, as it is clear from our theoretical investigation.
- Moreover, the current study also shows that the heat transfer capacity can be increased by 31.75%, 30.72% and 28.45% by dissolving SWCNTs, CuO, and TiO_2, respectively.
- The increases of φ will increase the viscosity of the Nanofluid, which leads to minimising the velocity profile.
- The increases of φ will increase the temperature distribution due to the increment of thermal conductivity of the nanofluid.

REFERENCES

[1] Verma, S. K., & Tiwari, A. K. (2015). Progress of nanofluid application in solar collectors: a review. Energy Conversion and Management, 100, 324-346.

[2] Javadi, F. S., Saidur, R., & Kamalisarvestani, M. (2013). Investigating performance improvement of solar collectors by using nanofluids. Renewable and Sustainable Energy Reviews, 28, 232-245.

[3] Suman, S., Khan, M. K., & Pathak, M. (2015). Performance enhancement of solar collectors—A review. Renewable and Sustainable Energy Reviews, 49, 192-210.

[4] Choi, S. U. S., Singer, D. A., & Wang, H. P. (1995). Developments and applications of non-Newtonian flows. Asme Fed, 66, 99-105.

[5] Khanafer, K., Vafai, K., & Lightstone, M. (2003). Buoyancy-driven heat transfer enhancement in a two-dimensional enclosure utilizing nanofluids. International journal of heat and mass transfer, 46(19), 3639-3653.

[6] Khaled, A. R., & Vafai, K. (2005). Heat transfer enhancement through control of thermal dispersion effects. International Journal of Heat and Mass Transfer, 48(11), 2172-2185.

[7] Khanafer, K., & Vafai, K. (2018). A review on the applications of nanofluids in solar energy field. Renewable Energy, 123, 398-406.

[8] Ramesh, G., & Prabhu, N. K. (2011). Review of thermo-physical properties, wetting and heat transfer characteristics of nanofluids and their applicability in industrial quench heat treatment. Nanoscale research letters, 6(1), 1-15.

[9] Khanafer, K., & Vafai, K. (2011). A critical synthesis of thermophysical characteristics of nanofluids. International journal of heat and mass transfer, 54(19-20), 4410-4428.

[10] Fan, J., & Wang, L. (2011). Review of heat conduction in nanofluids. Journal of heat transfer, 133(4).

[11] Vajjha, R. S., & Das, D. K. (2012). A review and analysis on influence of temperature and concentration of nanofluids on thermophysical properties, heat transfer and pumping power. International journal of heat and mass transfer, 55(15-16), 4063-4078.

[12] Trisaksri, V., & Wongwises, S. (2007). Critical review of heat transfer characteristics of nanofluids. Renewable and sustainable energy reviews, 11(3), 512-523.

[13] Daungthongsuk, W., & Wongwises, S. (2007). A critical review of convective heat transfer of nanofluids. Renewable and sustainable energy reviews, 11(5), 797-817.

[14] Kakaç, S., & Pramuanjaroenkij, A. (2009). Review of convective heat transfer enhancement with nanofluids. International journal of heat and mass transfer, 52(13-14), 3187-3196.

[15] Godson, L., Raja, B., Lal, D. M., & Wongwises, S. E. A. (2010). Enhancement of heat transfer using nanofluids—an overview. Renewable and sustainable energy reviews, 14(2), 629-641.
[16] Sarkar, J. (2011). A critical review on convective heat transfer correlations of nanofluids. Renewable and sustainable energy reviews, 15(6), 3271-3277.
[17] Ding, Y., Chen, H., Wang, L., Yang, C. Y., He, Y., Yang, W., ... & Huo, R. (2007). Heat transfer intensification using nanofluids. KONA Powder and Particle Journal, 25, 23-38.
[18] Kleinstreuer, C., Li, J., & Koo, J. (2008). Microfluidics of nano-drug delivery. International Journal of Heat and Mass Transfer, 51(23-24), 5590-5597.
[19] Öztop, H. F., Estellé, P., Yan, W. M., Al-Salem, K., Orfi, J., & Mahian, O. (2015). A brief review of natural convection in enclosures under localized heating with and without nanofluids. International Communications in Heat and Mass Transfer, 60, 37-44.
[20] Hussanan, A., Salleh, M. Z., Khan, I., & Shafie, S. (2017). Convection heat transfer in micropolar nanofluids with oxide nanoparticles in water, kerosene and engine oil. Journal of Molecular Liquids, 229, 482-488.
[21] Tesfai, W., Singh, P., Shatilla, Y., Iqbal, M. Z., & Abdala, A. A. (2013). Rheology and microstructure of dilute graphene oxide suspension. Journal of nanoparticle research, 15(10), 1-7.
[22] Ali, F., Gohar, M., & Khan, I. (2016). MHD flow of water-based Brinkman type nanofluid over a vertical plate embedded in a porous medium with variable surface velocity, temperature and concentration. Journal of Molecular Liquids, 223, 412-419.
[23] Wu, J. M., & Zhao, J. (2013). A review of nanofluid heat transfer and critical heat flux enhancement—research gap to engineering application. Progress in Nuclear Energy, 66, 13-24.
[24] Khan, I. (2017). Shape effects of MoS2 nanoparticles on MHD slip flow of molybdenum disulphide nanofluid in a porous medium. Journal of Molecular Liquids, 233, 442-451.
[25] Sheikholeslami, M., & Bhatti, M. M. (2017). Active method for nanofluid heat transfer enhancement by means of EHD. International Journal of Heat and Mass Transfer, 109, 115-122.
[26] Rashidi, M. M., Yang, Z., Awais, M., Nawaz, M., & Hayat, T. (2017). Generalized magnetic field effects in Burgers' nanofluid model. PLoS One, 12(1), e0168923.
[27] Mahian, O., Kianifar, A., Heris, S. Z., Wen, D., Sahin, A. Z., & Wongwises, S. (2017). Nanofluids effects on the evaporation rate in a solar still equipped with a heat exchanger. Nano Energy, 36, 134-155.
[28] Kasaeian, A., Daneshazarian, R., Mahian, O., Kolsi, L., Chamkha, A. J., Wongwises, S., & Pop, I. (2017). Nanofluid flow and heat transfer in porous media: a review of the latest developments. International Journal of Heat and Mass Transfer, 107, 778-791.
[29] Kalogirou, S. A. (2013). Solar energy engineering: processes and systems. Academic Press.
[30] Mahian, O., Kianifar, A., Kalogirou, S. A., Pop, I., & Wongwises, S. (2013). A review of the applications of nanofluids in solar energy. International Journal of Heat and Mass Transfer, 57(2), 582-594.
[31] Sheikh, N. A., Ali, F., Khan, I., Gohar, M., & Saqib, M. (2017). On the applications of nanofluids to enhance the performance of solar collectors: A comparative analysis of Atangana-Baleanu and Caputo-Fabrizio fractional models. The European Physical Journal Plus, 132(12), 1-11.
[32] Varol, Y., & Oztop, H. F. (2007). Buoyancy induced heat transfer and fluid flow inside a tilted wavy solar collector. Building and Environment, 42(5), 2062-2071.
[33] Fan, J., Shah, L. J., & Furbo, S. (2007). Flow distribution in a solar collector panel with horizontally inclined absorber strips. Solar energy, 81(12), 1501-1511.
[34] Hatami, M., Mosayebidorcheh, S., & Jing, D. (2017). Thermal performance evaluation of alumina-water nanofluid in an inclined direct absorption solar collector (IDASC) using numerical method. Journal of Molecular Liquids, 231, 632-639.
[35] Atangana, A., & Vermeulen, P. D. (2014, January). Analytical solutions of a space-time fractional derivative of groundwater flow equation. In Abstract and Applied Analysis (Vol. 2014). Hindawi.
[36] Oldham, K., & Spanier, J. (1974). The fractional calculus theory and applications of differentiation and integration to arbitrary order. Elsevier.
[37] Caputo, M. (1967). Linear models of dissipation whose Q is almost frequency independent—II. Geophysical Journal International, 13(5), 529-539.
[38] Machado, J. T., Galhano, A., & Trujillo, J. (2013). Science metrics on fractional calculus development since 1966. Fractional Calculus and Applied Analysis, 16(2), 479-500.
[39] Friedrich, C. H. R. (1991). Relaxation and retardation functions of the Maxwell model with fractional derivatives. Rheologica Acta, 30(2), 151-158.

[40] Ali, F., Jan, S. A. A., Khan, I., Gohar, M., & Sheikh, N. A. (2016). Solutions with special functions for time fractional free convection flow of Brinkman-type fluid. The European Physical Journal Plus, 131(9), 1-13.

[41] Xue, Q. Z. (2005). Model for thermal conductivity of carbon nanotube-based composites. Physica B: Condensed Matter, 368(1-4), 302-307.

[42] He, Y., Wang, S., Ma, J., Tian, F., & Ren, Y. (2011). Experimental study on the light-heat conversion characteristics of nanofluids. Nanoscience and Nanotechnology Letters, 3(4), 494-496.Nanoscience and Nanotechnology.

[43] Sheikh, N. A., Ching, D. L. C., Khan, I., Kumar, D., & Nisar, K. S. (2020). A new model of fractional Casson fluid based on generalized Fick's and Fourier's laws together with heat and mass transfer. Alexandria Engineering Journal, 59(5), 2865-2876.